

A Block-Iterative Surrogate Constraint Splitting Method for Quadratic Signal Recovery

Patrick L. Combettes, *Senior Member, IEEE*

Abstract—A block-iterative parallel decomposition method is proposed to solve general quadratic signal recovery problems under convex constraints. The proposed method proceeds by local linearizations of blocks of constraints and it is therefore not sensitive to their analytical complexity. In addition, it naturally lends itself to implementation on parallel computing architectures due to its flexible block-iterative structure. Comparisons with existing methods are carried out and the case of inconsistent constraints is also discussed. Numerical results are presented.

I. INTRODUCTION

Solving a signal recovery (restoration or reconstruction) problem as a convex feasibility problem consists of finding a signal \bar{x} in a suitable Hilbert space $(\mathcal{H}, \|\cdot\|)$ that satisfies all the convex constraints derived from *a priori* knowledge and from the observed data [12], [48], [52]. Quadratic constraints, i.e., constraints of the form $\|L_j x - r_j\|_j^2 \leq \xi_j$, where L_j is a linear operator from \mathcal{H} into a Hilbert space $(\mathcal{H}_j, \|\cdot\|_j)$ and r_j a signal in \mathcal{H}_j , have proven especially useful in a number of signal recovery applications, e.g., [12], [31], [34], [36], [41], [46], [48]. In some problems, however, reliable bounds $(\xi_j)_{1 \leq j \leq p}$ may not be available for p of the quadratic constraints. If $(S_i)_{i \in I}$ denotes the family of precisely defined constraint sets, a sensible option is then to find a signal \bar{x} in the “hard” feasibility set

$$S = \bigcap_{i \in I} S_i \quad (1)$$

that least violates the p uncertain quadratic constraints. This can be achieved by minimizing a weighted average of the functions $x \mapsto \|L_j x - r_j\|_j^2$ ($1 \leq j \leq p$) over S , i.e., by solving the following general quadratic signal recovery problem: given weights $(\alpha_j)_{1 \leq j \leq p}$ in $]0, +\infty[$,

find $\bar{x} \in S$ such that $J(\bar{x}) = \inf J(S)$,

$$\text{where } J: x \mapsto \sum_{j=1}^p \alpha_j \|L_j x - r_j\|_j^2. \quad (2)$$

Practically speaking, a solution to (2) is a feasible signal \bar{x} whose linear transformations $(L_j \bar{x})_{1 \leq j \leq p}$ are the closest, in a weighted least-squares sense, to the reference signals $(r_j)_{1 \leq j \leq p}$. This formulation, which naturally fits within the hard-constrained feasibility framework of [15], covers a broad spectrum of signal recovery problems. For instance, a minimum energy feasible signal is obtained by choosing $J: x \mapsto \|x\|^2$ in (2) [7], [38], [44]. More generally, (2) yields the

smoothest feasible signal relative to some high-pass filtering operator $L: \mathcal{H} \rightarrow \mathcal{H}$ with $J: x \mapsto \|Lx\|^2$ [31], [49], and the best feasible approximation to a reference signal $r \in \mathcal{H}$ with $J: x \mapsto \|x - r\|^2$ [9], [20], [49]. Other special cases of (2) arise in connection with noisy linear recovery problems, in which the observed signal y_1 lies in some Hilbert space $(\mathcal{H}_1, \|\cdot\|_1)$ and is related to the original signal x via the equation $y_1 = L_1 x + u_1$, where $L_1: \mathcal{H} \rightarrow \mathcal{H}_1$ is linear and $u_1 \in \mathcal{H}_1$ represents noise. In the absence of precise statistical information on $\|u_1\|_1^2$, it is customary to minimize over the feasibility set S the function $J: x \mapsto \|L_1 x - y_1\|_1^2$ [39] or, more generally, the function $J: x \mapsto \|L_1 x - y_1\|_1^2 + \gamma_1 \|M_1(x - r_1)\|^2$, where $M_1: \mathcal{H} \rightarrow \mathcal{H}$ is linear, $r_1 \in \mathcal{H}$, and $\gamma_1 \in [0, +\infty[$ [1], [7], [22], [29], [30], [47]. In other problems [23], [34], [40], q linear measurements of x , say $y_j = L_j x + u_j$ ($1 \leq j \leq q$), may have been recorded in unknown noise environments. In such instances, the quadratic objective will be extended to $J: x \mapsto \sum_{j=1}^q \beta_j \|L_j x - y_j\|_j^2 + \gamma_j \|M_j(x - r_j)\|^2$, where $(\beta_j)_{1 \leq j \leq q}$ are weights in $]0, +\infty[$.

In the literature, several methods can be found that solve (2) under certain conditions. In practice, however, these methods suffer from several limitations and they can seldom be implemented efficiently due to the specific challenges posed by signal recovery problems, which not only involve a sizable amount of data and unknowns, but also a wide variety of constraints that lead to intricate feasibility sets with no explicit analytical description. In this paper, we propose a new constrained quadratic minimization method that alleviates these limitations and is particularly well suited for large-scale signal recovery applications in the presence of complex convex constraints. The method is an adaptation of an outer approximation scheme recently proposed in [14]. It has a block-iterative parallel structure and can therefore fully take advantage of parallel processing architectures. Its computational efficiency is further enhanced by the fact that it does not require exact enforcement of the constraints but merely approximate enforcement by means of local linearizations.

The remainder of the paper consists of six sections. The assumptions and notation used in the paper are formally introduced in Section II. In Section III, existing quadratic minimization methods are reviewed and their limitations in the context of signal recovery applications are discussed. The new method is presented in Section IV. In Section V, the behavior of the algorithm in the presence of inconsistent constraints is analyzed. Numerical applications to signal deconvolution and image restoration are demonstrated in Section VI. Section VII concludes the paper. The proofs of our results have been placed in the Appendix.

Manuscript received December 30, 2001; revised January 4, 2003. This work was supported in part by the National Science Foundation under grant MIP-9705504. The associate editor coordinating the review of this paper and approving it for publication was Dr. A. H. Krim.

The author is with the Laboratoire Jacques-Louis Lions, Université Pierre et Marie Curie – Paris 6, 75005 Paris, France (e-mail plc@math.jussieu.fr).

Digital Object Identifier XXXX.

A. Notation

The signal space \mathcal{H} is a real Hilbert space with scalar product $\langle \cdot | \cdot \rangle$, norm $\| \cdot \|$, and distance d . The distance from a signal $x \in \mathcal{H}$ to a nonempty set $C \subset \mathcal{H}$ is $d_C(x) = \inf\{\|x - y\| \mid y \in C\}$. Given a continuous convex function $f: \mathcal{H} \rightarrow \mathbb{R}$ and $\eta \in \mathbb{R}$, the closed and convex set $\text{lev}_{\leq \eta} f = \{x \in \mathcal{H} \mid f(x) \leq \eta\}$ is the *lower level set* of f at height η . A vector $t \in \mathcal{H}$ is a *subgradient* of f at $x \in \mathcal{H}$ if the continuous affine function $y \mapsto \langle y - x | t \rangle + f(x)$, which coincides with f at x , minorizes f , i.e.,

$$(\forall y \in \mathcal{H}) \quad \langle y - x | t \rangle + f(x) \leq f(y). \quad (3)$$

Clearly,

$$0 \in \partial f(x) \Leftrightarrow f(x) = \inf f(\mathcal{H}). \quad (4)$$

As f is continuous, it always possesses at least one subgradient at each point x . If f happens to be (Gâteaux) differentiable at x , then it possesses a unique subgradient at this point which is simply its *gradient* $\nabla f(x)$. The set of all subgradients of f at x is the *subdifferential* of f at x and is denoted by $\partial f(x)$. Finally, a sequence $(x_n)_{n \geq 0}$ in \mathcal{H} converges to $x \in \mathcal{H}$ *strongly* if $(\|x_n - x\|)_{n \geq 0}$ converges to 0 and *weakly* if, for every $y \in \mathcal{H}$, $(\langle x_n - x | y \rangle)_{n \geq 0}$ converges to 0.

B. Subgradient projections

The reader is referred to [12], [13] for a tutorial account of subgradients and signal recovery examples (see also [17] and [51] for recent applications of these concepts and further examples). We provide here some essential facts.

Let C be a nonempty closed and convex subset of \mathcal{H} and let x be a point in \mathcal{H} . Then there exists a unique point $P_C x \in C$ such that $\|x - P_C x\| = d_C(x)$; $P_C x$ is the *projection* of x onto C and is characterized by

$$P_C x \in C \text{ and } (\forall y \in C) \quad \langle y - P_C x | x - P_C x \rangle \leq 0. \quad (5)$$

Computing the projection onto C amounts to solving a constrained quadratic minimization problem, which usually involves some iterative procedure. A notable exception is when one deals with a half-space, say $H = \{y \in \mathcal{H} \mid \langle y | u \rangle \leq \eta\}$, where $u \in \mathcal{H} \setminus \{0\}$ and $\eta \in \mathbb{R}$. The projection of x onto H is given explicitly by

$$P_H x = \begin{cases} x + \frac{\eta - \langle x | u \rangle}{\|u\|^2} u, & \text{if } \langle x | u \rangle > \eta; \\ x, & \text{if } \langle x | u \rangle \leq \eta. \end{cases} \quad (6)$$

Therefore, if C can be approximated at x by a half-space H_x , an economical approximation to $P_C x$ will be $P_{H_x} x$. We shall now describe a general context in which it is possible to do so.

Suppose $C = \text{lev}_{\leq 0} f \neq \emptyset$, where $f: \mathcal{H} \rightarrow \mathbb{R}$ is continuous and convex (this level set representation of a closed convex set is quite general since one can always put $C = \text{lev}_{\leq 0} d_C$). Fix $x \in \mathcal{H}$ and a subgradient $t \in \partial f(x)$. Then (3) provides a linearization of f at x and it implies that, if $f(y) \leq 0$, then $\langle y - x | t \rangle + f(x) \leq 0$. Now define

$$H_x = \begin{cases} \{y \in \mathcal{H} \mid \langle x - y | t \rangle \geq f(x)\}, & \text{if } f(x) > 0; \\ \mathcal{H}, & \text{if } f(x) \leq 0. \end{cases} \quad (7)$$

The projection of x onto H_x is a *subgradient projection* of x onto C . Observe that, if $f(x) > 0$, then $t \neq 0$ by (4) since $C \neq \emptyset$. Hence, it follows from (6) that

$$P_{H_x} x = \begin{cases} x - \frac{f(x)t}{\|t\|^2}, & \text{if } f(x) > 0; \\ x, & \text{if } f(x) \leq 0. \end{cases} \quad (8)$$

To sum up,

$$C \subset H_x = \{y \in \mathcal{H} \mid \langle y - P_{H_x} x | x - P_{H_x} x \rangle \leq 0\}. \quad (9)$$

We also note that if $f = d_C$ the notion of subgradient projection reverts to the usual notion of projection, i.e., $P_{H_x} x = P_C x$ [3, Rem. 7.6].

C. Assumptions

Our standing assumptions on the quadratic cost J in (2) will be the following.

- Assumption 1** $J: \mathcal{H} \rightarrow \mathbb{R}: x \mapsto \sum_{j=1}^p \alpha_j \|L_j x - r_j\|_j^2$, where
- for every $j \in \{1, \dots, p\}$, L_j is a continuous linear operator from \mathcal{H} into a real Hilbert space \mathcal{H}_j with norm $\| \cdot \|_j$, $r_j \in \mathcal{H}_j$, and $\alpha_j \in]0, +\infty[$;
 - L_1 has a continuous left inverse.

Some immediate consequences of these assumptions are recorded below.

- Proposition 2** (See Appendix) Let $R = \sum_{j=1}^p \alpha_j L_j^* L_j: \mathcal{H} \rightarrow \mathcal{H}$, where L_j^* denotes the adjoint of L_j . Then
- R is bounded and continuously invertible.
 - The form $\langle \cdot | \cdot \rangle_R: \mathcal{H}^2 \rightarrow \mathbb{R}: (x, y) \mapsto \langle Rx | y \rangle$ is a scalar product on \mathcal{H} .
 - The norm $\| \cdot \|_R: x \mapsto \sqrt{\langle Rx | x \rangle}$ associated with $\langle \cdot | \cdot \rangle_R$ is equivalent to $\| \cdot \|$.

Definition 3 \mathcal{H}_R is the Hilbert space obtained by renorming \mathcal{H} with the norm $\| \cdot \|_R$ of Proposition 2.

Our assumptions on the feasibility set in (1) will be essentially the same as in [13] and [15].

Assumption 4 $S = \bigcap_{i \in I} S_i$, where:

- I is a finite or countably infinite index set.
- For every $i \in I$, $S_i = \text{lev}_{\leq 0} f_i \neq \emptyset$, where $f_i: \mathcal{H} \rightarrow \mathbb{R}$ is convex and continuous.

III. EXISTING SOLUTION METHODS

Throughout this section it is assumed that the problem is consistent, i.e., $S \neq \emptyset$.

A. Equivalent best approximation problem

The analysis of Problem (2) is greatly simplified by the following fact, which establishes an equivalence between (2) and a projection problem in the alternate Hilbert space \mathcal{H}_R .

Proposition 5 (See Appendix) Let $r = R^{-1} \sum_{j=1}^p \alpha_j L_j^* r_j$. Then

- i) $(\forall x \in \mathcal{H}) \quad J(x) = \|x - r\|_R^2 - \|r\|_R^2 + \sum_{j=1}^p \alpha_j \|r_j\|_j^2$.
ii) *Problem (2) is equivalent to projecting r onto S in \mathcal{H}_R , i.e., to*

$$\text{find } \bar{x} \in S \text{ such that } (\forall x \in S) \quad \|\bar{x} - r\|_R \leq \|x - r\|_R. \quad (10)$$

- iii) *Problem (2) admits a unique solution \bar{x} , which is characterized by the variational inequality*

$$\bar{x} \in S \text{ and } (\forall x \in S) \quad \left\langle x - \bar{x} \left| \sum_{j=1}^p \alpha_j L_j^* (r_j - L_j \bar{x}) \right. \right\rangle \leq 0. \quad (11)$$

B. General overview

Several algorithms have been proposed in the signal recovery literature that can solve (10) and, therefore, (2) in specific cases. Thus, the algorithm of [39] is restricted to a nonnegativity constraint whereas the approach of [20] provides a finite parameterization for linear data models which it is limited in practice to simple constraints, as projections onto the feasibility set S are required (the same limitation is also found in the projected gradient method of [15] and the projected Landweber method of [22]). On the other hand, the algorithm of [38] is restricted to minimum norm problems with two sets and is numerically demanding.

In the quadratic programming literature, algorithms have been proposed for certain types of constraint sets such as half-spaces, cones, affine subspaces, hyperslabs (see [9] and the references therein). To our knowledge, there are two main parallel methods to solve (10) in the general context defined by Assumptions 1 and 4. We shall now review these two methods and comment on their numerical limitations. Hereafter, $(P_i)_{i \in I}$ and $(P_i^R)_{i \in I}$ denote the projectors onto the sets $(S_i)_{i \in I}$ in the spaces \mathcal{H} and \mathcal{H}_R , respectively, and $(\omega_i)_{i \in I}$ are strictly positive weights such that $\sum_{i \in I} \omega_i = 1$. The structure of these methods will be seen to be akin to that of the parallel projection method (PPM)

$$x_0 = r \text{ and } (\forall n \in \mathbb{N}) \quad x_{n+1} = \sum_{i \in I} \omega_i P_i^R x_n, \quad (12)$$

which is known to converge weakly to an undetermined point in S in general [13], and to converge strongly to the solution \bar{x} of (10) if $(S_i)_{i \in I}$ is a family of closed vector subspaces [37] (see also [43]). The parallelism of this method stems from the fact that the projections $(P_i^R x_n)_{i \in I}$ can be computed simultaneously.

C. Dykstra's algorithm

Dykstra's algorithm was originally proposed in [21] and [5] as a periodic POCS-like scheme with modified projection operators to solve (10) with I finite [9]. A parallel version of this algorithm was subsequently developed in [24] (see also [2] and [32]), which takes the following form in \mathcal{H}_R .

Algorithm 6 $x_0 = r$, $(\forall i \in I) \quad z_{i,0} = x_0$, and for every $n \in \mathbb{N}$

$$\begin{cases} x_{n+1} = \sum_{i \in I} \omega_i P_i^R z_{i,n} \\ (\forall i \in I) \quad z_{i,n+1} = x_{n+1} + (z_{i,n} - P_i^R z_{i,n}). \end{cases} \quad (13)$$

Algorithm 6 differs from (12) in that for every $i \in I$ the vector $z_{i,n} - P_i^R z_{i,n}$ (the outward normal to S_i at $P_i^R z_{i,n}$) generated at iteration n is added to the next iterate x_{n+1} before projecting onto S_i . If all the S_i 's are closed affine subspaces, however, $P_i^R z_{i,n} = P_i^R x_n$ and (13) reverts to (12) [9].

Theorem 7 [2], [24] *Suppose I is finite. Then the sequence generated by Algorithm 6 converges strongly to the solution \bar{x} of (10).*

D. Anchor point method

The first anchor point method was proposed in [27] for minimum norm problems. Parallel versions were devised in [10], [11], and [12] for best approximation problems and recently extended to more general quadratic problems in [50].

Algorithm 8 $x_0 = \gamma Rr$ and for every $n \in \mathbb{N}$

$$x_{n+1} = \kappa_n x_0 + (\text{Id} - \kappa_n \gamma R) \left(x_n + \lambda \left(\sum_{i \in I} \omega_i P_i x_n - x_n \right) \right), \quad (14)$$

where $\gamma \in]0, 2/\|R\| [$, $\lambda \in]0, 2]$, and $(\kappa_n)_{n \geq 0}$ is a sequence in $[0, 1]$ such that

$$\begin{cases} \lim_{n \rightarrow +\infty} \kappa_n = 0 \\ \sum_{n \geq 0} \kappa_n = +\infty \\ \sum_{n \geq 0} |\kappa_{n+1} - \kappa_n| < +\infty. \end{cases} \quad (15)$$

As n becomes large, κ_n tends to 0 and the influence of the ‘‘anchor point’’ x_0 fades away, making the iteration process (14) increasingly similar to (12) when $R = \text{Id}$ and $\lambda = \gamma = 1$.

Theorem 9 (See Appendix) *Every sequence $(x_n)_{n \geq 0}$ generated by Algorithm 8 converges strongly to the solution \bar{x} of (10).*

IV. PROPOSED SURROGATE CONSTRAINT SPLITTING ALGORITHM

The proposed algorithm, which is an off-spring of a general outer approximation scheme for constrained convex minimization recently proposed in [14], aims at alleviating the shortcomings of the methods discussed in Section III. We continue to assume that $S \neq \emptyset$. The following notation will be convenient.

Definition 10 *Given $(u, v, w) \in \mathcal{H}^3$ such that*

$$A = \{y \in \mathcal{H} \mid \langle y - v \mid u - v \rangle_R \leq 0\} \\ \cap \{y \in \mathcal{H} \mid \langle y - w \mid v - w \rangle_R \leq 0\} \neq \emptyset,$$

$Q^R(u, v, w)$ denotes the projection of u onto A in \mathcal{H}_R , i.e., $Q^R(u, v, w) = P_A^R u$.

A. Geometrical construction

When faced with a complex minimization problem, a common strategy in optimization is to try and replace it by a sequence of simpler problems. The proposed method adopts this strategy and its principle is to decompose (2) into a sequence of minimization problems over simple outer approximations $(A_n)_{n \geq 0}$ to the feasibility set S , which is split into its elementary components $(S_i)_{i \in I}$.

The algorithm is initialized with $x_0 = r$ and, at iteration $n \in \mathbb{N}$, the outer approximation A_n is constructed as the intersection of (at most) two closed half-spaces containing S . More specifically, $A_n = D_n \cap H_n$, where

$$\begin{aligned} D_n &= \{y \in \mathcal{H} \mid \langle x_n - y \mid \nabla J(x_n) \rangle \leq 0\} \\ &= \{y \in \mathcal{H} \mid \langle y - x_n \mid x_0 - x_n \rangle_R \leq 0\} \end{aligned} \quad (16)$$

and

$$H_n = \{y \in \mathcal{H} \mid \langle y - z_n \mid x_n - z_n \rangle_R \leq 0\}. \quad (17)$$

The point z_n is chosen so that H_n contains the intersection of a finite block of constraint sets $(S_i)_{i \in I_n}$, where the set of indices $I_n \subset I$ is chosen by the user. H_n is called a *surrogate half-space* (or *cut*) for the block $(S_i)_{i \in I_n}$. The update x_{n+1} is then computed as the minimizer of J over A_n , i.e., by Proposition 5i),

$$x_{n+1} = Q^R(x_0, x_n, z_n). \quad (18)$$

This process is depicted in Fig. 1. An essential feature of this algorithm is that the subproblem (18) is straightforward to solve, as shown below.¹

Lemma 11 [14, Eq. (6.9)] *Set $\pi_n = \langle x_0 - x_n \mid x_n - z_n \rangle_R$, $\mu_n = \|x_0 - x_n\|_R^2$, $\nu_n = \|x_n - z_n\|_R^2$, and $\rho_n = \mu_n \nu_n - \pi_n^2$. Then*

$$Q^R(x_0, x_n, z_n) = \begin{cases} z_n, & \text{if } \rho_n = 0 \text{ and } \pi_n \geq 0; \\ x_0 + (1 + \pi_n/\nu_n)(z_n - x_n), & \text{if } \rho_n > 0 \text{ and } \pi_n \nu_n \geq \rho_n; \\ x_n + \frac{\nu_n}{\rho_n} (\pi_n(x_0 - x_n) + \mu_n(z_n - x_n)), & \text{if } \rho_n > 0 \text{ and } \pi_n \nu_n < \rho_n. \end{cases} \quad (19)$$

Let us now discuss the construction of H_n , i.e., how to define z_n in (17) so that $\bigcap_{i \in I_n} S_i \subset H_n$. For every $i \in I_n$, we first compute a subgradient projection $p_{i,n}$ of x_n onto S_i via (8), i.e.,

$$p_{i,n} = \begin{cases} x_n - \frac{f_i(x_n)t_{i,n}}{\|t_{i,n}\|^2}, & t_{i,n} \in \partial f_i(x_n), \text{ if } f_i(x_n) > 0; \\ x_n, & \text{if } f_i(x_n) \leq 0. \end{cases} \quad (20)$$

As seen in (9), the set

$$S_{i,n} = \{y \in \mathcal{H} \mid \langle y - p_{i,n} \mid x_n - p_{i,n} \rangle \leq 0\} \quad (21)$$

¹This lemma is essentially [28, Thm. 3-1], which also states that $(\rho_n = 0 \text{ and } \pi_n < 0) \Leftrightarrow D_n \cap H_n = \emptyset$. Note that since $\rho_n \geq 0$ (Cauchy-Schwarz) and $\emptyset \neq S \subset D_n \cap H_n$ in our construction, all the possible cases are therefore exhausted in (19).

serves as an outer approximation to $S_i = \text{lev}_{\leq 0} f_i$. Hence, if $(\omega_{i,n})_{i \in I_n}$ are nonnegative weights adding up to one, the inequality $\sum_{i \in I_n} \omega_{i,n} \langle y - p_{i,n} \mid x_n - p_{i,n} \rangle \leq 0$ is a surrogate for the block of inequalities $\max_{i \in I_n} f_i(y) \leq 0$ at x_n and the half-space $\tilde{H}_n = \{y \in \mathcal{H} \mid \sum_{i \in I_n} \omega_{i,n} \langle y - p_{i,n} \mid x_n - p_{i,n} \rangle \leq 0\}$ serves as an outer approximation to $\bigcap_{i \in I_n} S_i$. Now define

$$u_n = x_n - \sum_{i \in I_n} \omega_{i,n} p_{i,n} \quad \text{and} \quad L_n = \begin{cases} \frac{\sum_{i \in I_n} \omega_{i,n} \|p_{i,n} - x_n\|^2}{\langle R^{-1}u_n \mid u_n \rangle}, & \text{if } x_n \notin \bigcap_{i \in I_n} S_i; \\ 1/\|R^{-1}\|, & \text{otherwise.} \end{cases} \quad (22)$$

Proposition 12 (See Appendix) $L_n \geq 1/\|R^{-1}\|$.

For more flexibility, instead of \tilde{H}_n , we shall actually use the relaxed half-space

$$H_n = \left\{ y \in \mathcal{H} \mid \sum_{i \in I_n} \omega_{i,n} \langle y - p_{i,n} \mid x_n - p_{i,n} \rangle \leq (L_n - \lambda_n) \langle R^{-1}u_n \mid u_n \rangle \right\}, \quad (23)$$

where the relaxation parameter λ_n lies in $[\varepsilon L_n, L_n]$, for some $\varepsilon \in]0, 1[$. We are now ready to evaluate z_n in (17).

Proposition 13 (See Appendix) $z_n = P_{H_n}^R x_n = x_n - \lambda_n R^{-1}u_n$.

In summary, the proposed algorithm for constructing a sequence $(x_n)_{n \geq 0}$ of approximate solutions to (2) can be described as follows.

Algorithm 14

- ① Fix $\varepsilon \in]0, 1[$. Set $x_0 = r$ and $n = 0$.
- ② Take a nonempty finite index set $I_n \subset I$.
- ③ Set $z_n = x_n + \lambda_n R^{-1} (\sum_{i \in I_n} \omega_{i,n} p_{i,n} - x_n)$, where
 - a) for every $i \in I_n$, $p_{i,n}$ is as in (20);
 - b) $(\omega_{i,n})_{i \in I_n}$ lies in $[0, 1]$ and $\sum_{i \in I_n} \omega_{i,n} = 1$;
 - c) $\lambda_n \in [\varepsilon L_n, L_n]$, where L_n is as in (22).
- ④ Compute $x_{n+1} = Q^R(x_0, x_n, z_n)$ via (19).
- ⑤ Set $n = n + 1$ and go to ②.

B. Convergence

The following mild conditions will be imposed on the index control sequence $(I_n)_{n \geq 0}$, the weights $((\omega_{i,n})_{i \in I_n})_{n \geq 0}$, the relaxation parameters $(\lambda_n)_{n \geq 0}$, and the subdifferentials $(\partial f_i)_{i \in I}$.

Assumption 15

- i) For every $i \in I$, there exists a strictly positive integer M_i such that, for every $n \in \mathbb{N}$, $i \in \bigcup_{k=n}^{n+M_i-1} I_k$.
- ii) There exists $\delta \in]0, 1[$ such that, for every $n \in \mathbb{N}$,

$$(\exists j \in I_n) \begin{cases} \|p_{j,n} - x_n\| = \max_{i \in I_n} \|p_{i,n} - x_n\| \\ \omega_{j,n} \geq \delta. \end{cases} \quad (24)$$

iii) *There exists $z \in S$ such that, for every $i \in I$, the set $\partial f_i(\text{lev}_{\leq J(z)} J)$ is bounded.*

Let us briefly comment on this set of assumptions.

- Condition i) imposes that every index i be used at least once within any M_i consecutive iterations, M_i being left to the user's choice. This control rule provides great flexibility in the management of the constraints and the implementation of the algorithm. Specific examples are supplied in [12], [13].
- Condition ii) asks that the weight assigned to one of the subgradient projections that induces the maximum step be bounded away from zero.
- Condition iii) asks that the subdifferential of each f_i be bounded on a lower level set of J intersecting with the feasibility set S . Since the lower level sets of J are bounded, iii) is satisfied under the standard assumption that ∂f_i maps bounded sets into bounded sets, which is always true in finite dimensional spaces [6, Thm. 9.2.3].

Theorem 16 (See Appendix) *Suppose Assumption 15 is satisfied. Then every sequence $(x_n)_{n \geq 0}$ generated by Algorithm 14 converges strongly to the solution \bar{x} of (10).*

Two special cases of this theorem can be found in [33] and [42], where they were obtained via a different analysis. In [42, Thm. V.1], I is finite, $R = \text{Id}$, $I_n \equiv I$, $\lambda_n \equiv L_n$, $\omega_{i,n} \equiv 1/\text{card } I$, and exact projections are required, i.e., $f_i = d_{S_i}$. In [33, Thm. 3], $\dim \mathcal{H} < +\infty$, I is finite, $R = \text{Id}$, $I_n \equiv I$, $\lambda_n \equiv L_n$, and $\omega_{i,n} \equiv \omega_i$.

C. Implementation

In best approximation problems and, in particular, in minimum norm problems, $R = \text{Id}$. In general quadratic problems, however, since the operators R and R^{-1} appear in several places in Algorithm 14, it is important to organize the computations so as to minimize their use. By executing the n th iteration as indicated below, it is possible to apply R and R^{-1} only once.

- For every $i \in I_n$, set $a_i = -f_i(x_n)t_i/\|t_i\|^2$, where $t_i \in \partial f_i(x_n)$, if $f_i(x_n) > 0$; $a_i = 0$ otherwise.²
- Choose convex weights $(\omega_i)_{i \in I_n}$ conforming to (24). Set $v = \sum_{i \in I_n} \omega_i a_i$ and $L = \sum_{i \in I_n} \omega_i \|a_i\|^2$.
- If $L = 0$, set $x_{n+1} = x_n$ and exit iteration. Otherwise, set $b = x_0 - x_n$, $c = Rb$, $d = R^{-1}v$, and $L = L/\langle d | v \rangle$.
- Choose $\lambda \in [\varepsilon L, L]$ and set $d = \lambda d$.
- Set $\pi = -\langle c | d \rangle$, $\mu = \langle b | c \rangle$, $\nu = \lambda \langle d | v \rangle$, and $\rho = \mu\nu - \pi^2$.
- Set $x_{n+1} = \begin{cases} x_n + d, & \text{if } \rho = 0 \text{ and } \pi \geq 0; \\ x_0 + (1 + \pi/\nu)d, & \text{if } \rho > 0 \text{ and } \pi\nu \geq \rho; \\ x_n + \frac{\nu}{\rho}(\pi b + \mu d), & \text{if } \rho > 0 \text{ and } \pi\nu < \rho. \end{cases}$

D. Discussion

In view of Theorems 7, 9, and 16, Algorithms 6, 8, and 14 all produce sequences $(x_n)_{n \geq 0}$ converging strongly to the solution of (10) and, therefore, of (2) by Proposition 5ii). Nonetheless, they differ in important respects.

²Recall from Section II-B that if the projection $P_i x_n$ of x_n onto S_i is easy to compute, one can set $f_i = d_{S_i}$, which yields $a_i = P_i x_n - x_n$.

• Algorithms 6 and 8 have a static parallel structure in that all the sets must be activated at each iteration with constant weights. As a result, if the number of sets exceeds the number of available concurrent processors, the implementation will not be optimal. By contrast, Algorithm 14 has the ability to process variable blocks of constraints. It is therefore possible to closely match the computational load of each iteration to the parallel processing architecture at hand. More details on the importance of block-processing for task scheduling on parallel architectures will be found in [8].

- Algorithm 6 demands that auxiliary vectors $(z_{i,n})_{i \in I}$ be stored at each iteration, which complicates its implementation in terms of memory allocation and management.
- Algorithm 6 operates with the projectors $(P_i^R)_{i \in I}$. Implementing such operators amounts to solving costly quadratic subproblems. For instance, if $x \notin S_i$ and f_i is differentiable on S_i with $\text{lev}_{< 0} f_i \neq \emptyset$, a straightforward application of the Karush-Kuhn-Tucker Theorem [53, Thm. 47.E(2)] shows that $P_i^R x$ is obtained by solving the system

$$P_i^R x = x - \lambda R^{-1} \nabla f_i(P_i^R x), \quad f_i(P_i^R x) = 0, \quad \lambda > 0 \quad (25)$$

for $(P_i^R x, \lambda)$. This system has no closed-form solution in general and represents in itself a nontrivial optimization problem that must typically be solved iteratively.³ Algorithm 8 is somewhat less demanding as it employs the natural projectors $(P_i)_{i \in I}$ (whence $R = \text{Id}$ in (25)). In comparison, a decisive advantage of Algorithm 14 is that it activates the constraints via approximate (subgradient) projections rather than exact projections. The former are significantly easier to implement than the latter, as they require only the computation of subgradients (gradients in the differentiable case) in the original space \mathcal{H} (see (20)) as opposed to solving (25). Analytically complex constraints can therefore be incorporated in the recovery algorithm and processed at low cost.

Additional attractive features of Algorithm 14 are listed below:

- In other optimization problems, surrogate half-spaces of type (23) have been reported to induce deep cuts and to yield algorithms with very good convergence speeds [12], [13], [25], [26], [35].
- It possesses a convenient stopping rule, namely feasibility: $x_n = \bar{x} \Leftrightarrow x_n \in S$ [14, Prop. 3.1(v)].
- It allows for the weights and the relaxations to vary at each iteration.
- It can handle a countably infinite number of constraints.

It follows from the above discussion that, overall, Algorithm 14 emerges as the most flexible and efficient method to solve (2).

We close this section by observing that Algorithm 14 is closely related to the EMOPSP algorithm of [13]: EMOPSP is obtained for $R = \text{Id}$ by replacing c) in Step ③ by “ $\lambda_n \in [\varepsilon, (2 - \varepsilon)L_n]$ ” and Step ④ by “Set $x_{n+1} = z_n$ ”. Note, however, that under Assumption 15 EMOPSP guarantees only weak convergence to an unspecified signal in S [13, Thm. 3] rather than strong convergence to the solution of (2) (see also [4] for deeper insights).

³In the nondifferentiable case, the problem is even more involved as $P_i^R x = (\text{Id} + R^{-1} \lambda \partial f_i)^{-1}(x)$, where λ is any solution in $]0, +\infty[$ of the equation $f_i(P_i^R x) = 0$.

In some problems, the feasibility set S may turn out to be empty due to conflicting constraints. Such situations may be caused, for instance, by inaccurate deterministic constraints, by overly aggressive confidence levels on stochastic constraints, or by inadequate data modeling (see [10], [15], and the references therein).

In this section we discuss the behavior of the algorithms of Sections III and IV when $S = \emptyset$. Our working assumptions are as follows.

Assumption 17

- i) I is finite.
- ii) For some $i \in I$, S_i is bounded.
- iii) $\{\omega_i\}_{i \in I} \subset]0, 1]$ and $\sum_{i \in I} \omega_i = 1$.

In [10], it was proposed to replace the (possibly empty) feasibility set S by the set G of signals that best approximate the constraints in a weighted least square-distance sense, that is

$$G = \left\{ x \in \mathcal{H} \mid (\forall y \in \mathcal{H}) \sum_{i \in I} \omega_i d_{S_i}(x)^2 \leq \sum_{i \in I} \omega_i d_{S_i}(y)^2 \right\}. \quad (26)$$

By virtue of Assumption 17, G is nonempty, closed, convex, and bounded and, if $S \neq \emptyset$, then $G = S$ [10, Prop. 7]. Thus, Problem (2) can be restated as

$$\begin{aligned} \text{find } \bar{x} \in G \text{ such that } J(\bar{x}) = \inf J(G), \\ \text{where } J: x \mapsto \sum_{j=1}^p \alpha_j \|L_j x - r_j\|_j^2. \end{aligned} \quad (27)$$

As in Proposition 5, it possesses a unique solution, namely, $P_G^R r$, the projection of $r = R^{-1} \sum_{j=1}^p \alpha_j L_j^* r_j$ onto G in \mathcal{H}_R .

In general, the orbits of Algorithm 14 will not converge to the solution of (27) when $S = \emptyset$. We shall therefore consider a variant of this algorithm.

Algorithm 18

- ① Fix $\varepsilon \in]0, 1[$. Set $x_0 = r$ and $n = 0$.
- ② Set $v_n = \sum_{i \in I} \omega_i P_i x_n - x_n$ and $\Lambda_n = \begin{cases} \|v_n\|^2 / \langle R^{-1} v_n \mid v_n \rangle, & \text{if } x_n \notin G; \\ 1 / \|R^{-1}\|, & \text{otherwise.} \end{cases}$
- ③ Set $z_n = x_n + \lambda_n R^{-1} v_n$, where $\lambda_n \in [\varepsilon \Lambda_n, \Lambda_n]$.
- ④ Compute $x_{n+1} = Q^R(x_0, x_n, z_n)$ via (19).
- ⑤ Set $n = n + 1$ and go to ②.

Theorem 19 (See Appendix) *Let $(x_n)_{n \geq 0}$ be an arbitrary sequence generated by any of the following:*

- i) Algorithm 6.
- ii) Algorithm 8.
- iii) Algorithm 18.

Then $(x_n)_{n \geq 0}$ converges strongly to the solution \bar{x} of (27).

Algorithms 6, 8, and 18 are similar to the extent that they use exact projections and have a static parallel structure. Algorithms 8 and 18 are nonetheless easier to implement because they require only projections in \mathcal{H} (as opposed to \mathcal{H}_R) and do

not impose the storage of auxiliary vectors. Let us also note that, for $R = \text{Id}$, the PPM algorithm (12) is obtained by altering Algorithm 18 as follows: use the relaxation interval $[\varepsilon, 2 - \varepsilon]$ in lieu of $[\varepsilon \Lambda_n, \Lambda_n] = [\varepsilon, 1]$ in Step ③, and replace Step ④ by “Set $x_{n+1} = z_n$ ”. Under Assumption 17, PPM guarantees only weak convergence to an unspecified signal in G [10, Thm. 4] whereas Algorithm 18 secures strong convergence to the solution of (27).

VI. NUMERICAL EXAMPLES

We compare the numerical performance of the proposed Algorithm 14 with that of Algorithms 6 and 8. The algorithms have been tested on various other signal and image recovery (denoising, reconstruction, restoration) problems, with similar conclusions.

A. Signal deconvolution

We revisit a benchmark digital signal deconvolution problem arising in spectroscopy and initially proposed in [48].

A.1 Experiment

The N -point ($N = 1024$) emission spectrum x shown in Fig. 2 is blurred by convolution with a Gaussian impulse response with mean zero and a standard deviation of 28 points. The degraded signal y shown in Fig. 3 is obtained by adding uniformly distributed i.i.d. noise to the blurred signal. The noise range is $[-\xi, \xi]$, where $\xi = 0.5$. The signal space \mathcal{H} is the standard Euclidean space \mathbb{R}^N and $(e_i)_{0 \leq i \leq N-1}$ denotes its canonical basis. The degradation model is $y = Lx + u$, where the blurring matrix L and the distribution of the entries of the noise vector u are assumed to be known. The blurred signal-to-noise ratio is $20 \log_{10}(\|Lx\|/\|u\|) = 7.56$ dB. For reference, the Wiener filtering solution for this problem is displayed in Fig. 4.

The following closed convex constraint sets considered in [48] are used:

- $S_1 = \bigcap_{i=0}^{N-1} \{z \in \mathcal{H} \mid \langle z \mid e_i \rangle \geq 0\}$ is the set of nonnegative signals.
- $S_2 = \{z \in \mathcal{H} \mid \|y - Lz\|^2 \leq \zeta\}$ is the set of signals producing a residual whose sample second moment is consistent with that of the noise. Here L is the impulse response matrix and the bound ζ is computed so as to yield a 95 percent confidence level (see [18] for details).
- $(S_i)_{3 \leq i \leq N+2}$ are the sets of signals producing a residual whose pointwise amplitude is consistent with that of the noise, i.e.,

$$S_i = \{z \in \mathcal{H} \mid |\langle y - Lz \mid e_{i-3} \rangle| \leq \xi\}. \quad (28)$$

The set of feasible signals is $S = \bigcap_{i=1}^{N+2} S_i$. A feasible solution is shown in Fig. 5. Clearly, the feasibility set defined on the basis of the above constraints contains unsatisfactory solutions due to the low SNR and the severity of the blur. Next, we approach this problem via (2) with $L_1 = \text{Id}$, $L_2 = \nabla = \text{circ}([1, 0, \dots, 0, -1])$ (first order, circulant, finite-difference matrix), $r_1 = r_2 = 0$, and $\alpha_1 = \alpha_2 = 1$. The quadratic recovery problem (2) therefore amounts to finding the smoothest feasible signal relative to the discrete Sobolev H^1 -norm, which yields $r = 0$ and $R = \text{circ}([3, -1, 0, \dots, 0, -1])$ in the equivalent formulation (10). The solution \bar{x} to this problem is the signal shown in Fig. 6.

A.2 Projections

The projectors P_1 and $(P_i)_{3 \leq i \leq N+2}$ can be obtained in closed form [12] and will therefore be used by all algorithms. On the other hand, the projectors P_2^R and P_2 must be implemented iteratively [48]. Since Algorithms 6 and 8 require exact projections, they must activate S_2 by means of P_2^R and P_2 , respectively. By contrast, Algorithm 14 can activate S_2 by means of subgradient projections, which is much more economical computationally. Indeed, the subgradient projection of x_n onto S_2 is simply

$$p_{2,n} = \begin{cases} x_n + \frac{\|q_n\|^2 - \zeta}{2\|L^*q_n\|^2} L^*q_n, & \text{if } \|q_n\|^2 > \zeta; \\ x_n, & \text{otherwise;} \end{cases} \quad (29)$$

where $q_n = y - Lx_n$, and it can be computed in the DFT domain efficiently [13].

A.3 Numerical performance

The algorithms are run on a computer with eight parallel processors. The products involving the dense circulant matrix R^{-1} are computed with the FFT. Specific details concerning the implementation follow.

- **Dykstra's algorithm:** Algorithm 6 is implemented with equal weights $(\omega_i)_{1 \leq i \leq 1026}$ on the projections.
- **Anchor point method:** Algorithm 8 is implemented with $\gamma = 1/\|R\|$, $\lambda = 1.9$, and $\kappa_n = 1/(2+n)$. Moreover, equal weights $(\omega_i)_{1 \leq i \leq 1026}$ are used on the projections.
- **Proposed method:** The index control sequence $(I_n)_{n \geq 0}$ of Algorithm 14 is designed so as to sweep through the sets in conformity with Assumption 15i). At iteration n , I_n selects the following block of sets: S_1 , S_2 , and b_n consecutive sets in (28), starting with S_j ($3 \leq j \leq N+2$ modulo N), where S_{j-1} is the last set used at iteration $n-1$. The number b_n is determined so that the block contains $l_n = \min\{8, m_n\}$ violated constraints, where m_n is the total number of violated constraints. The weight is $\omega_{i,n} = 1/l_n$ on each violated constraint and $\omega_{i,n} = 0$ on the nonviolated ones (Assumption 15ii) is thus satisfied). Each violated constraint is assigned to a separate processor. Finally, the relaxation parameter is set to be $\lambda_n = L_n$. In view of Proposition 13, this relaxation parameter maximizes $\|z_n - x_n\|_R = d_{H_n^R}^R(x_n)$, i.e., the depth of the cut generated by the surrogate half-space H_n . This maximal relaxation strategy has been found to yield faster convergence consistently (this observation about the superiority of large relaxations in parallel (subgradient) projection algorithms concurs with those made for convex feasibility algorithms in [12], [13], [25], [26], [35]).

The figure of merit used to compare the algorithms in Fig. 7 is the normalized mean square error $\|x_n - \bar{x}\|^2 / \|\bar{x}\|^2$ in terms of the combined CPU time n (expressed in arbitrary units). Note that an iteration of Algorithm 14 requires merely the computation of 8 subgradient projections whereas an iteration of Algorithms 6 and 8 requires the computation of $N+2 = 1026$ exact projections. It would therefore not be meaningful to compare the algorithms in terms of iteration count. For this reason, we use actual CPU time to give a direct assessment of the computational load of the algorithms. As seen in Fig. 7, the proposed method, which uses subgradient projections and efficient block-iterative cuts, is extremely fast compared with Dykstra's algorithm and the anchor point method. Dykstra's algorithm, which

must compute the projections in \mathcal{H}_R and manage $N+2 = 1026$ outer normals, is actually significantly slower than the anchor point method.

B. Image restoration

We consider a digital image restoration problem similar to those of [12], [13], and [48].

B.1 Experiment

The $N \times N$ -point ($N = 128$) original image x shown in Fig. 8 is blurred by convolution with a uniform rectangular 7×7 kernel. The degraded image y shown in Fig. 9 is obtained by adding zero mean Gaussian white noise to the blurred image, with a blurred image-to-noise ratio of 30.0 dB. Using standard column stacking for the images, the signal space \mathcal{H} is the standard Euclidean space \mathbb{R}^{N^2} . Thus, $y = Lx + u$, where the point spread function matrix L and the distribution of the entries of the noise vector u are assumed to be known. For reference, the Wiener filtering solution for this problem is displayed in Fig. 10.

Four constraint sets are used in this experiment.

- S_1 is the set of nonnegative images.
- $S_2 = \{z \in \mathcal{H} \mid \|y - Lz\|^2 \leq \zeta\}$ is the set of images producing a residual whose sample second moment is consistent with that of the noise.
- $S_3 = \{z \in \mathcal{H} \mid |\langle y - Lz \mid \underline{1} \rangle| \leq \chi\}$ is the set of images producing a residual whose sample mean is consistent with that of the noise ($\underline{1}$ is the vector whose entries are all equal to 1).
- S_4 is the set of images producing a residual whose periodogram is consistent with that of the noise, i.e.,

$$S_4 = \bigcap_{(k,l) \in D} \{z \in \mathcal{H} \mid |\widehat{|y - Lz|}^2(k,l)| \leq \xi\}, \quad (30)$$

where $D = \{1, \dots, N/2 - 1\} \times \{1, \dots, N - 1\}$ and $\widehat{\cdot}$ stands for the 2-D DFT.

The bounds ζ , χ , and ξ are computed so as to yield a 98.33 percent confidence level on the sets S_2 , S_3 , and S_4 , respectively (see [12, Section VI.D.2] and [18] for details). Following the analysis of [16], the global confidence level on the feasibility set $S = S_1 \cap S_2 \cap S_3 \cap S_4$ is 95 percent. Because the only *a priori* information about the true image is nonnegativity, S contains rough images, such as that displayed in Fig. 11. To select a smoother feasible image, we look for a minimal energy solution, which amounts to taking $r = 0$ and $J: x \mapsto \|x\|^2$ in (2). The solution \bar{x} to this problem is shown in Fig. 12.

B.2 Projections

The projectors P_1 , P_3 , and P_4 can be obtained in closed form and are therefore used by all algorithms. Expressions for P_1 and P_4 can be found in [12] and, for every $z \in \mathcal{H}$, [12, Eq. (2.24)] yields

$$P_3 z = \begin{cases} z + \frac{\langle y - Lz \mid \underline{1} \rangle - \chi}{\|d\|^2} d, & \text{if } \langle y - Lz \mid \underline{1} \rangle > \chi; \\ z, & \text{if } |\langle y - Lz \mid \underline{1} \rangle| \leq \chi; \\ z + \frac{\langle y - Lz \mid \underline{1} \rangle + \chi}{\|d\|^2} d, & \text{if } \langle y - Lz \mid \underline{1} \rangle < -\chi; \end{cases} \quad (31)$$

where $d = L^* \underline{1}$. On the other hand, as in Section VI-A.2, S_2 will be activated via the subgradient projection (29) in Algorithm 14, whereas Algorithms 6 and 8 must use the exact projector P_2 .

B.3 Numerical performance

The algorithms are implemented on a 4-processor machine. This experiment is much more favorable to Algorithms 6 and 8 than the previous one since the number of processors matches exactly the number of constraints. Hence, all three algorithms can be efficiently implemented in parallel by assigning one (sub-gradient) projection to each processor at each iteration.

• **Dykstra’s algorithm:** Equal weights $(\omega_i)_{1 \leq i \leq 4}$ are used on the projections.

• **Anchor point method:** As in Section VI-A.3, Algorithm 8 is implemented with $\gamma = 1/\|R\|$, $\lambda = 1.9$, $\kappa_n = 1/(2+n)$, and equal weights $(\omega_i)_{1 \leq i \leq 4}$ on the projections.

• **Proposed method:** At every iteration n of Algorithm 14, $I_n = I$ and $\lambda_n = L_n$.

Fig. 13 shows the value of the normalized mean square error $\|x_n - \bar{x}\|^2 / \|\bar{x}\|^2$ versus the combined CPU time n (expressed in arbitrary units). The proposed method is seen to be faster than Dykstra’s algorithm and the anchor point method. Here, however, Dykstra’s algorithm performs better than the anchor point method. This better performance is due to the fact that, since $J = \|\cdot\|^2$, $R = \text{Id}$ and standard projections can therefore be used. In addition, the low number of constraints makes the management of the outer normals much less demanding than in the previous experiment.

VII. CONCLUSION

Quadratic objectives arise in a variety of signal recovery problems. We have proposed an efficient algorithm to solve such problems under very general assumptions on the underlying constraints. The algorithm possesses two distinguishing features that make it more attractive than existing quadratic minimization methods. First, it can easily be implemented on modern parallel computing architectures due to its flexible block-iterative structure. Second, it relies on a surrogate constraint scheme that allows for the local linearization of complex convex constraints. This algorithm complements the EMOPSP method of [13], which features the same block-iterative surrogate constraints handling capabilities but is limited to feasibility problems.

APPENDIX A – PROOFS

The standard facts from linear functional analysis used below can be found in [19] and [45].

Proof of Proposition 2: Let x be an arbitrary point in \mathcal{H} . i): It follows from Assumption 1i) that the operators $(L_j)_{j \leq p}$ are bounded. Upon defining $\eta_2 = \sum_{j=1}^p \alpha_j \|L_j\|^2$, we get

$$\|Rx\| \leq \sum_{j=1}^p \alpha_j \|L_j^* L_j x\| \leq \sum_{j=1}^p \alpha_j \|L_j^* L_j\| \cdot \|x\| = \eta_2 \|x\|. \quad (32)$$

Hence R is bounded. Furthermore, it follows from Assumption 1ii) that there exists a constant $\beta_1 \in]0, +\infty[$, independent

from x , such that $\|L_1 x\|_1^2 \geq \beta_1 \|x\|^2$ [45, p. 420]. Now let $\eta_1 = \alpha_1 \beta_1$. Then, by Cauchy-Schwarz,

$$\begin{aligned} \eta_1 \|x\|^2 &\leq \alpha_1 \|L_1 x\|_1^2 \leq \sum_{j=1}^p \alpha_j \|L_j x\|_j^2 \\ &= \sum_{j=1}^p \alpha_j \langle L_j^* L_j x \mid x \rangle = \langle Rx \mid x \rangle \leq \|Rx\| \cdot \|x\|. \end{aligned} \quad (33)$$

Hence, $\|Rx\| \geq \eta_1 \|x\|$ and R is therefore continuously invertible. ii): Since R is self-adjoint, $\langle \cdot \mid \cdot \rangle_R$ is a symmetric bilinear form. Moreover, by (33), $\langle x \mid x \rangle_R \geq 0$ and $\langle x \mid x \rangle_R = 0 \Leftrightarrow x = 0$. Thus, $\langle \cdot \mid \cdot \rangle_R$ is a scalar product. iii): Combining (32) and (33), we get $\eta_1 \|x\|^2 \leq \|x\|_R^2 \leq \eta_2 \|x\|^2$, i.e., the norms $\|\cdot\|$ and $\|\cdot\|_R$ are equivalent. ■

Proof of Proposition 5: i): Let x be an arbitrary point in \mathcal{H} and put $\eta = \sum_{j=1}^p \alpha_j \|r_j\|_j^2$. Then, since R^{-1} is self-adjoint,

$$\begin{aligned} J(x) - \eta &= \sum_{j=1}^p \alpha_j \|L_j x - r_j\|_j^2 - \eta \\ &= \sum_{j=1}^p \alpha_j (\|L_j x\|_j^2 - 2\langle L_j x \mid r_j \rangle_j) \\ &= \sum_{j=1}^p \alpha_j (\langle L_j^* L_j x \mid x \rangle - 2\langle x \mid L_j^* r_j \rangle) \\ &= \langle Rx \mid x \rangle - 2\langle Rx \mid R^{-1} \sum_{j=1}^p \alpha_j L_j^* r_j \rangle \\ &= \|x - r\|_R^2 - \|r\|_R^2. \end{aligned} \quad (34)$$

i) \Rightarrow ii): Clear. ii) \Rightarrow iii): Since S is a nonempty closed convex set, \bar{x} exists, is unique, and, by (5), is characterized by $\bar{x} \in S$ and $(\forall x \in S) \langle x - \bar{x} \mid r - \bar{x} \rangle_R \leq 0$, that is, by (11). ■

Lemma 20 [50, Thm. 2]: *Let $T: \mathcal{H} \rightarrow \mathcal{H}$ be a nonexpansive⁴ operator such that $\text{Fix } T = \{x \in \mathcal{H} \mid Tx = x\} \neq \emptyset$ and let $M: \mathcal{H} \rightarrow \mathcal{H}$ be a bounded, self-adjoint, strongly positive⁵ operator such that $\|\text{Id} - M\| < 1$. Let $x_0 \in \mathcal{H}$, let $(\kappa_n)_{n \geq 0}$ be a sequence in $[0, 1]$ that satisfies (15), and set*

$$(\forall n \in \mathbb{N}) \quad x_{n+1} = \kappa_n x_0 + (\text{Id} - \kappa_n M) T x_n. \quad (35)$$

Then $(x_n)_{n \geq 0}$ converges strongly to the unique minimizer of $f: x \mapsto \langle Mx \mid x \rangle - 2\langle x \mid x_0 \rangle$ over $\text{Fix } T$.

Proof of Theorem 9: Let $T = \text{Id} + \lambda(\sum_{i \in I} \omega_i P_i - \text{Id})$ and $M = \gamma R$ in Lemma 20. Then the iterative scheme (14) is equivalent to (35). Let us now show that T and M meet the required conditions. First, by combining arguments of [10] and [11], we get that T is nonexpansive with $\text{Fix } T = S$. Next, since R is linear, bounded (by Proposition 2i)), self-adjoint, and strongly positive (by (33)), so is M . Now let $U = \{x \in \mathcal{H} \mid \|x\| = 1\}$. Then, by self-adjointness, $\|R\| = \sup_{x \in U} |\langle Rx \mid x \rangle|$. Hence, for every $x \in U$, (33) $\Rightarrow \eta_1 \leq \langle Rx \mid x \rangle \leq \|R\| \Rightarrow -1 + (2 - \gamma\|R\|) \leq 1 - \gamma\langle Rx \mid x \rangle \leq 1 - \gamma\eta_1 \Rightarrow$

⁴ $(\forall (x, y) \in \mathcal{H}^2) \|Tx - Ty\| \leq \|x - y\|$.

⁵ $(\exists \alpha \in]0, +\infty[) (\forall x \in \mathcal{H}) \langle Mx \mid x \rangle \geq \alpha \|x\|^2$.

$|1 - \gamma \langle Rx | x \rangle| \leq 1 - \min\{2 - \gamma \|R\|, \gamma \eta_1\} < 1$. Consequently, $\|\text{Id} - M\| = \sup_{x \in U} |\langle x - \gamma Rx | x \rangle| = \sup_{x \in U} |1 - \gamma \langle Rx | x \rangle| < 1$. Furthermore, upon setting $x_0 = \gamma Rr$, we get $(\forall x \in \mathcal{H}) \|x - r\|_R^2 = (f(x)/\gamma) + \langle Rr | r \rangle$. Hence, minimizing $\|\cdot - r\|_R$ over $\text{Fix } T$ is equivalent to minimizing J over S and the result follows from Lemma 20. ■

Proof of Proposition 12: We first observe that L_n is well defined since [14, Prop. 4.5]

$$x_n \in \bigcap_{i \in I_n} S_i \Leftrightarrow u_n = 0. \quad (36)$$

It is enough to assume $x_n \notin \bigcap_{i \in I_n} S_i$. By convexity of $\|\cdot\|^2$, $\sum_{i \in I_n} \omega_{i,n} \|p_{i,n} - x_n\|^2 / \|u_n\|^2 \geq 1$. On the other hand, since R^{-1} is strictly positive, the Cauchy-Schwarz inequality yields $0 < \langle R^{-1}u_n | u_n \rangle \leq \|R^{-1}\| \cdot \|u_n\|^2$. Altogether, $L_n = (\sum_{i \in I_n} \omega_{i,n} \|p_{i,n} - x_n\|^2 / \|u_n\|^2) (\|u_n\|^2 / \langle R^{-1}u_n | u_n \rangle) \geq 1 / \|R^{-1}\|$. ■

Proof of Proposition 13: Let us first rewrite (23) as

$$H_n = \{y \in \mathcal{H} \mid \langle y | u_n \rangle \leq \eta_n\}, \text{ where} \\ \eta_n = \sum_{i \in I_n} \omega_{i,n} \langle p_{i,n} | x_n - p_{i,n} \rangle + (L_n - \lambda_n) \langle R^{-1}u_n | u_n \rangle. \quad (37)$$

If $x_n \in \bigcap_{i \in I_n} S_i$, then (20) implies that, for all $i \in I_n$, $p_{i,n} = x_n$ and, in turn, that $H_n = \mathcal{H}$. The claim is therefore trivial. We now assume $x_n \notin \bigcap_{i \in I_n} S_i$. Using the characterization (5), it is easy to verify that

$$P_{H_n}^R x_n = \begin{cases} x_n + \frac{\eta_n - \langle x_n | u_n \rangle}{\langle R^{-1}u_n | u_n \rangle} R^{-1}u_n, & \text{if } \langle x_n | u_n \rangle > \eta_n; \\ x_n, & \text{if } \langle x_n | u_n \rangle \leq \eta_n. \end{cases} \quad (38)$$

Replacing u_n and η_n by their values we therefore obtain $P_{H_n}^R x_n = x_n - \lambda_n R^{-1}u_n$. Since, in view of (5) and (17), $z_n = P_{H_n}^R x_n$, the proof is complete. ■

Proof of Theorem 16: We apply [14, Thm. 6.4(i)]. First let us note that, by virtue of Proposition 5, we can consider that the objective in Problem (2) is $x \mapsto \langle Rx | x \rangle / 2 - \langle x | Rr \rangle$. Hence, it follows from (33), [14, Prop. 2.1(iii)], Assumption 4, and [14, Prop. 2.2(ii)] that assumptions [14, (A1)–(A3)] are satisfied with $E = \mathcal{H}$. Next, we observe that, since $\varepsilon L_n \leq \lambda_n \leq L_n$, it follows from (22) that (23) can be written as

$$H_n = \left\{ y \in \mathcal{H} \mid \sum_{i \in I_n} \omega_{i,n} \langle y - p_{i,n} | x_n - p_{i,n} \rangle \leq \gamma_n \right\}, \quad (39)$$

where $0 \leq \gamma_n \leq (1 - \varepsilon) \sum_{i \in I_n} \omega_{i,n} \|p_{i,n} - x_n\|^2$. In view of Assumption 15ii), Algorithm 14 is therefore a special case of [14, Algorithm 6.4]. Since by Assumption 15i)&iii) and [14, Prop. 4.7(ii)] all the conditions of [14, Thm. 6.4(i)] are fulfilled, the proof is complete. ■

Proof of Theorem 19: Put $T = \sum_{i \in I} \omega_i P_i$. Then [10]⁶

$$T \text{ is firmly nonexpansive and } \text{Fix } T = G. \quad (40)$$

i): [2, Thm. 6.1] (see also [32, Section 5] for the finite dimensional case). ii): Identical to the proof of Theorem 9 since (40) yields $\text{Fix} (\text{Id} + \lambda(\sum_{i \in I} \omega_i P_i - \text{Id})) = G$. iii): We apply [14, Thm. 6.4(i)], considering once again that the objective in Problem (27) is $x \mapsto \langle Rx | x \rangle / 2 - \langle x | Rr \rangle$. To this end, fix $n \in \mathbb{N}$ and let $H_n = \{y \in \mathcal{H} \mid \langle y - z_n | x_n - z_n \rangle_R \leq 0\}$. Then the identities $z_n = x_n + \lambda_n R^{-1}v_n$ and $v_n = Tx_n - x_n$, together with the inequalities $\varepsilon \Lambda_n \leq \lambda_n \leq \Lambda_n$ yield

$$H_n = \{y \in \mathcal{H} \mid \langle y - z_n | -v_n \rangle \leq 0\} \\ = \{y \in \mathcal{H} \mid \langle y - Tx_n | -v_n \rangle \leq \langle Tx_n - z_n | v_n \rangle\} \\ = \{y \in \mathcal{H} \mid \langle y - Tx_n | -v_n \rangle \leq (\Lambda_n - \lambda_n) \langle R^{-1}v_n | v_n \rangle\} \\ = \{y \in \mathcal{H} \mid \langle y - Tx_n | x_n - Tx_n \rangle \leq \gamma_n\}, \quad (41)$$

where $0 \leq \gamma_n \leq (1 - \varepsilon) \|Tx_n - x_n\|^2$. Therefore, it follows from (33), [14, Prop. 2.1(iii)], (40), and [14, (4.10) & Example 4.3] that Algorithm 18 is a special case of [14, Algorithm 6.4] with $E = \mathcal{H}$ and one set, namely $\text{Fix } T$. On the other hand, by (40) and [14, Prop. 4.7(iii)], all the conditions of [14, Thm. 6.4(i)] are fulfilled. The announced result is thus proved. ■

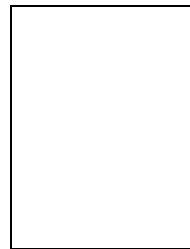
REFERENCES

- [1] E. Artzy, T. Elfving, and G. T. Herman, "Quadratic optimization for image reconstruction II," *Comput. Graph. Image Processing*, vol. 11, pp. 242–261, 1979.
- [2] H. H. Bauschke and J. M. Borwein, "Dykstra's alternating projection algorithm for two sets," *J. Approx. Theory*, vol. 79, pp. 418–443, 1994.
- [3] H. H. Bauschke and J. M. Borwein, "On projection algorithms for solving convex feasibility problems," *SIAM Rev.*, vol. 38, pp. 367–426, Sept. 1996.
- [4] H. H. Bauschke and P. L. Combettes, "A weak-to-strong convergence principle for Fejér-monotone methods in Hilbert spaces," *Math. Oper. Res.*, vol. 26, pp. 248–264, May 2001.
- [5] J. P. Boyle and R. L. Dykstra, "A method for finding projections onto the intersection of convex sets in Hilbert spaces," *Lecture Notes Statist.*, vol. 37, pp. 28–47, 1986.
- [6] J. M. Borwein and A. S. Lewis, *Convex Analysis and Nonlinear Optimization—Theory and Examples*. New York: Springer-Verlag, 2000.
- [7] Y. Censor, "Finite series-expansion reconstruction methods," *Proc. IEEE*, vol. 71, pp. 409–419, Mar. 1983.
- [8] Y. Censor and S. A. Zenios, *Parallel Optimization: Theory, Algorithms and Applications*. New York: Oxford University Press, 1997.
- [9] P. L. Combettes, "Signal recovery by best feasible approximation," *IEEE Trans. Image Processing*, vol. 2, pp. 269–271, Apr. 1993.
- [10] P. L. Combettes, "Inconsistent signal feasibility problems: Least-squares solutions in a product space," *IEEE Trans. Signal Processing*, vol. 42, pp. 2955–2966, Nov. 1994.
- [11] P. L. Combettes, "Construction d'un point fixe commun à une famille de contractions fermes," *C. R. Acad. Sci. Paris Sér. I Math.*, vol. 320, pp. 1385–1390, June 1995.
- [12] P. L. Combettes, "The convex feasibility problem in image recovery," in *Advances in Imaging and Electron Physics* (P. Hawkes, Ed.), vol. 95, pp. 155–270. New York: Academic Press, 1996.
- [13] P. L. Combettes, "Convex set theoretic image recovery by extrapolated iterations of parallel subgradient projections," *IEEE Trans. Image Processing*, vol. 6, pp. 493–506, Apr. 1997.
- [14] P. L. Combettes, "Strong convergence of block-iterative outer approximation methods for convex optimization," *SIAM J. Control Optim.*, vol. 38, pp. 538–565, Feb. 2000.

⁶An operator $T: \mathcal{H} \rightarrow \mathcal{H}$ is firmly nonexpansive if

$$(\forall (x, y) \in \mathcal{H}^2) \|Tx - Ty\|^2 \leq \|x - y\|^2 - \|(T - \text{Id})x - (T - \text{Id})y\|^2.$$

- [15] P. L. Combettes and P. Bondon, "Hard-constrained inconsistent signal feasibility problems," *IEEE Trans. Signal Processing*, vol. 47, pp. 2460–2468, Sept. 1999.
- [16] P. L. Combettes and T. J. Chaussalet, "Combining statistical information in set theoretic estimation," *IEEE Signal Processing Lett.*, vol. 3, pp. 61–62, Mar. 1996.
- [17] P. L. Combettes and J. Luo, "An adaptive level set method for nondifferentiable constrained image recovery," *IEEE Trans. Image Processing*, vol. 11, pp. 1295–1304, Nov. 2002.
- [18] P. L. Combettes and H. J. Trussell, "The use of noise properties in set theoretic estimation," *IEEE Trans. Signal Processing*, vol. 39, pp. 1630–1641, July 1991.
- [19] F. Deutsch, *Best Approximation in Inner Product Spaces*. New York: Springer-Verlag, 2001.
- [20] S. Dharanipragada and K. S. Arun, "A quadratically convergent algorithm for convex set constrained signal recovery," *IEEE Trans. Signal Processing*, vol. 44, pp. 248–266, Feb. 1996.
- [21] R. L. Dykstra, "An algorithm for restricted least squares regression," *J. Amer. Statist. Assoc.*, vol. 78, pp. 837–842, Dec. 1983.
- [22] B. Eicke, "Iteration methods for convexly constrained ill-posed problems in Hilbert space," *Numer. Funct. Anal. Optim.*, vol. 13, pp. 413–429, 1992.
- [23] M. Elad and A. Feuer, "Restoration of a single superresolution image from several blurred, noisy, and undersampled measured images," *IEEE Trans. Image Processing*, vol. 6, pp. 1646–1658, Dec. 1997.
- [24] N. Gaffke and R. Mathar, "A cyclic projection algorithm via duality," *Metrika*, vol. 36, pp. 29–54, 1989.
- [25] U. M. García-Palomares and F. J. González-Castaño, "Incomplete projection algorithms for solving the convex feasibility problem," *Numer. Algorithms*, vol. 18, pp. 177–193, 1998.
- [26] F. J. González-Castaño, U. M. García-Palomares, J. L. Alba-Castro, and J. M. Pousada-Carballo, "Fast image recovery using dynamic load balancing in parallel architectures, by means of incomplete projections," *IEEE Trans. Image Processing*, vol. 10, pp. 493–499, Apr. 2001.
- [27] B. Halpern, "Fixed points of nonexpanding maps," *Bull. Amer. Math. Soc.*, vol. 73, pp. 957–961, Nov. 1967.
- [28] Y. Haugazeau, *Sur les Inéquations Variationnelles et la Minimisation de Fonctionnelles Convexes*. Thèse, Université de Paris, Paris, France, 1968.
- [29] G. T. Herman and A. Lent, "Quadratic optimization for image reconstruction I," *Comput. Graph. Image Processing*, vol. 5, pp. 319–332, 1976.
- [30] B. R. Hunt, "The inverse problem of radiography," *Math. Biosciences*, vol. 8, pp. 161–179, June 1970.
- [31] B. R. Hunt, "The application of constrained least-squares estimation to image restoration by digital computer," *IEEE Trans. Computers*, vol. 22, pp. 805–812, Sept. 1973.
- [32] A. N. Iusem and A. R. De Pierro, "On the convergence of Han's method for convex programming with quadratic objective," *Math. Programming*, vol. 52, pp. 265–284, Aug. 1991.
- [33] A. N. Iusem and B. F. Svaiter, "A row-action method for convex programming," *Math. Programming*, vol. 64, pp. 149–171, 1994.
- [34] A. K. Katsaggelos, "A multiple input image restoration approach," *J. Visual Comm. Image Represent.*, vol. 1, pp. 93–103, Sept. 1990.
- [35] K. C. Kiwiel, "Monotone Gram matrices and deepest surrogate inequalities in accelerated relaxation methods for convex feasibility problems," *Linear Algebra Appl.*, vol. 252, pp. 27–33, Feb. 1997.
- [36] H. Kudo and T. Saito, "Sinogram recovery with the method of convex projections for limited-data reconstruction in computed tomography," *J. Opt. Soc. Amer.*, vol. A8, pp. 1148–1160, July 1991.
- [37] M. Lapidus, "Généralisation de la formule de Trotter-Lie," *C. R. Acad. Sci. Paris Sér. A Math.*, vol. 291, pp. 497–500, Oct. 1980.
- [38] R. M. Leahy and C. E. Goutis, "An optimal technique for constraint-based image restoration and reconstruction," *IEEE Trans. Acoust., Speech, Signal Processing*, vol. 34, pp. 1629–1642, Dec. 1986.
- [39] A. J. Levy, "A fast quadratic programming algorithm for positive signal restoration," *IEEE Trans. Acoust., Speech, Signal Processing*, vol. 31, pp. 1337–1341, Dec. 1983.
- [40] M. K. Ng and W. C. Kwan, "Comments on 'Least squares restoration of multichannel images'," *IEEE Trans. Signal Processing*, vol. 49, p. 2885, Nov. 2001.
- [41] P. Oskoui-Fard and H. Stark, "Tomographic image reconstruction using the theory of convex projections," *IEEE Trans. Med. Imaging*, vol. 7, pp. 45–58, Mar. 1988.
- [42] G. Pierra, "Éclatement de contraintes en parallèle pour la minimisation d'une forme quadratique," *Lecture Notes in Comput. Sci.*, vol. 41, pp. 200–218, 1976; See also "Decomposition through formalization in a product space," *Math. Programming*, vol. 28, pp. 96–115, Jan. 1984.
- [43] S. Reich, "A limit theorem for projections," *Linear and Multilinear Algebra*, vol. 13, pp. 281–290, 1983.
- [44] A. Sabharwal and L. C. Potter, "Convexly constrained linear inverse problems: Iterative least-squares and regularization," *IEEE Trans. Signal Processing*, vol. 46, pp. 2345–2352, Sept. 1998.
- [45] L. Schwartz, *Analyse—Topologie Générale et Analyse Fonctionnelle*, 2nd ed. Paris: Hermann, 1980.
- [46] M. I. Sezan and H. J. Trussell, "Prototype image constraints for set-theoretic image restoration," *IEEE Trans. Signal Processing*, vol. 39, pp. 2275–2285, Oct. 1991.
- [47] D. M. Titterton, "General structure of regularization procedures in image reconstruction," *Astron. Astrophys.*, vol. 144, pp. 381–387, Mar. 1985.
- [48] H. J. Trussell and M. R. Civanlar, "The feasible solution in signal restoration," *IEEE Trans. Acoust., Speech, Signal Processing*, vol. 32, pp. 201–212, Apr. 1984.
- [49] S. Twomey, "The application of numerical filtering to the solution of integral equations encountered in indirect sensing measurements," *J. Franklin Inst.*, vol. 279, pp. 95–109, Feb. 1965.
- [50] I. Yamada, N. Ogura, Y. Yamashita, and K. Sakaniwa, "Quadratic optimization of fixed points of nonexpansive mappings in Hilbert space," *Numer. Funct. Anal. Optim.*, vol. 19, pp. 165–190, 1998.
- [51] I. Yamada, K. Slavakis, and K. Yamada, "An efficient robust adaptive filtering algorithm based on parallel subgradient projection techniques," *IEEE Trans. Signal Processing*, vol. 50, pp. 1091–1101, May 2002.
- [52] D. C. Youla and H. Webb, "Image restoration by the method of convex projections: Part 1—Theory," *IEEE Trans. Medical Imaging*, vol. 1, pp. 81–94, Oct. 1982.
- [53] E. Zeidler, *Nonlinear Functional Analysis and Its Applications III: Variational Methods and Optimization*. New York: Springer-Verlag, 1985.



Patrick Louis Combettes (S'84-M'90-SM'96) is a Professor with the Laboratoire Jacques-Louis Lions, Université Pierre et Marie Curie – Paris 6, Paris, France.
Dr. Combettes is recipient of the IEEE Signal Processing Society Paper Award.

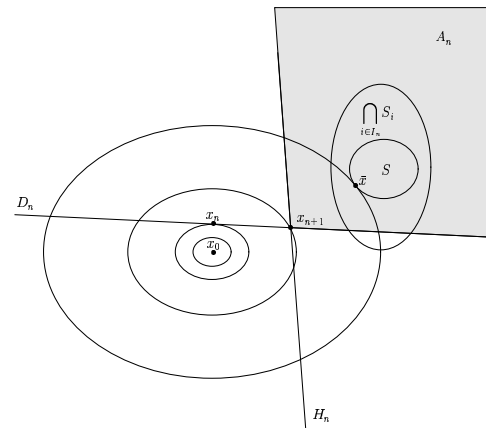


Fig. 1. Proposed algorithm: The ellipses centered at x_0 are the level curves of the objective function J and $x_{n+1} = P_{A_n}^R x_0$ minimizes J over the shaded area $A_n = D_n \cap H_n$.

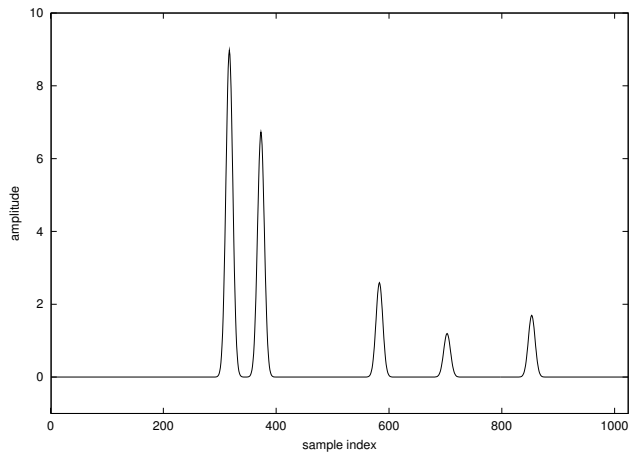


Fig. 2. Original signal.

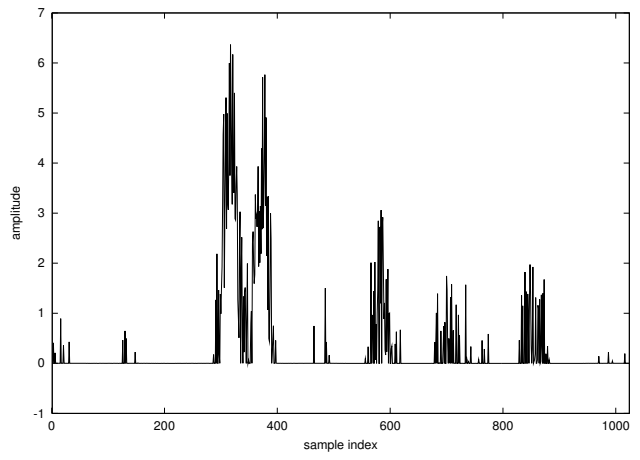


Fig. 5. A feasible signal.

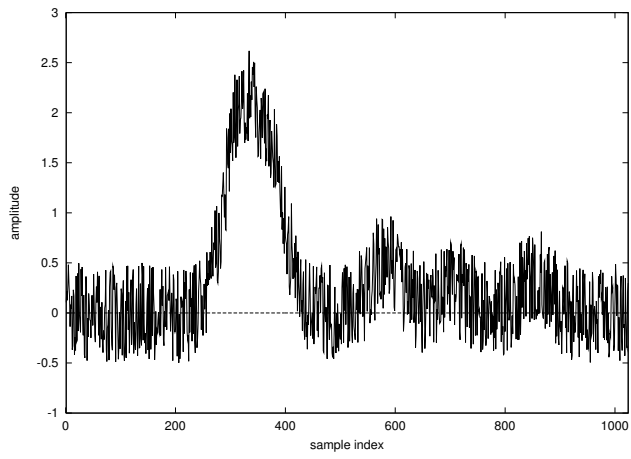


Fig. 3. Degraded signal.

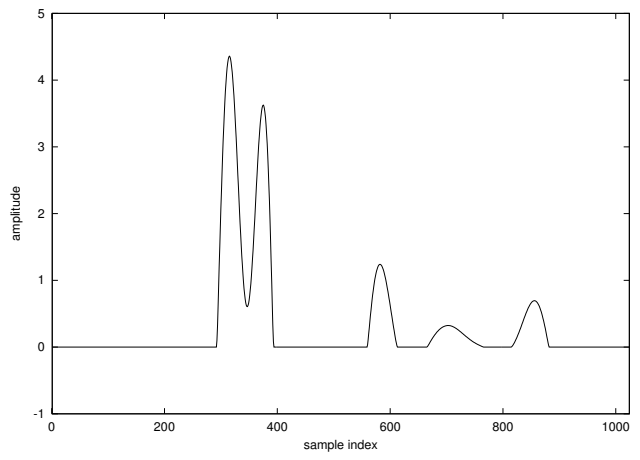


Fig. 6. Optimal quadratic solution \bar{x} .

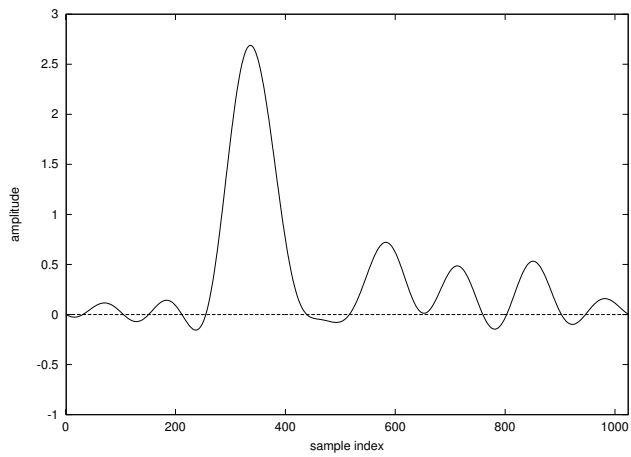


Fig. 4. Deconvolution by Wiener filtering.

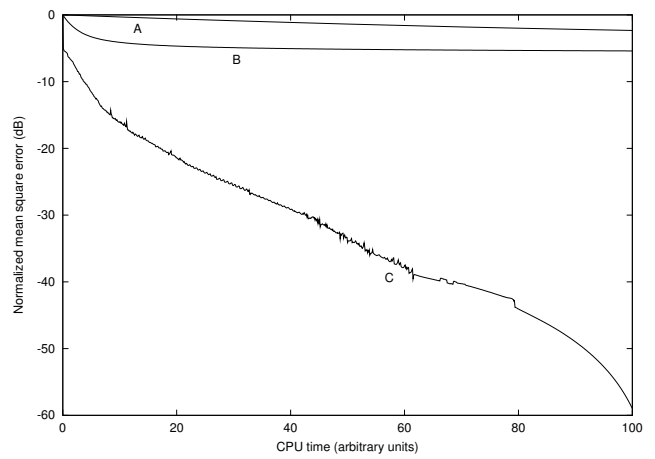


Fig. 7. Convergence patterns. A: Dykstra's algorithm; B: anchor point method; C: proposed method.



Fig. 8. Original image.



Fig. 11. A feasible image.



Fig. 9. Degraded image.



Fig. 12. Optimal minimum energy solution \bar{x} .



Fig. 10. Wiener filtering restoration.

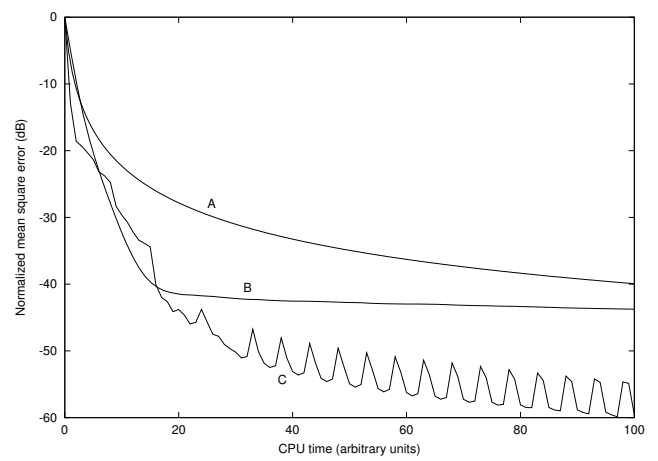


Fig. 13. Convergence patterns. A: anchor point method; B: Dykstra's algorithm; C: proposed method.